Application of the central-particle-potential approximation for percolation in interacting systems

A. Drory and I. Balberg
The Racah Institute of Physics, The Hebrew University, Jerusalem 91904, Israel

B. Berkowitz
Hydrological Service, Water Commission, Ministry of Agriculture, P.O. Box 6381, Jerusalem 91063, Israel
(Received 3 May 1995)

We compute the percolation threshold of systems of interacting particles by a random-adding algorithm with a rejection criterion based on the density distribution of the particles. The results are very close to those obtained in our previous work based on a simple Boltzmann central-particle approximation. The results are also essentially the same as those obtained by the Metropolis method, even though our algorithm is conceptually different and does not generate a true equilibrium configuration. This finding suggests that connectivity, in comparison with other system properties, is more "general" and is not sensitive to the particulars of the equilibrium state. Thus, our findings offer an efficient method for obtaining percolation thresholds in systems of interacting particles. This method is computationally simpler and faster than the well known Metropolis method.

PACS number(s): 02.70.−c, 64.60.Ak, 61.20.Ja, 82.70.Kj

I. INTRODUCTION

In a recent Rapid Communication [1] we reported an alternative method for computing percolation thresholds in systems of interacting particles. We argued that in comparison with the Metropolis algorithm used thus far for such problems, our random-adding method is more efficient and more natural to percolation problems. In the present paper we extend our comparison of the two methods, starting with a system of particles having a repulsive "hard core"and a connective "soft shell." The percolation thresholds obtained by the two methods are practically identical. This fact is remarkable because it contrasts sharply with the situation for other equilibrium properties (such as the pair-correlation function), where the random-adding procedure and the Metropolis algorithm are known to disagree [1]. Thus, it may be simpler to simulate connectivity properties than thermodynamic properties.

Following these conclusions we have generalized our method to other more complex interactions, by providing a rejection criterion which mimics some global features of the equilibrium configuration of the system. Basically, our criterion ensures that, e.g., in the presence of an attractive "well," particles will tend to conglomerate around each other. The results obtained by this method are in excellent agreement with those obtained by the Metropolis algorithm. This has two consequences: First, it confirms the usefulness of the random-adding algorithm as a more efficient tool for computing percolation thresholds. Second, it confirms that connectivity properties require only some global features of the equilibrium configuration, which are apparently the ones contained in our rejection criterion. This also explains the success of our previous method, the heuristic Boltzmann central-particle approximation, which turns out to be a simplified version of the more rigorous criterion provided here.

The rest of this paper is organized as follows: In Sec. II we present the problem of percolation thresholds in the continuum with interparticle interactions. In Sec. III we compare the Metropolis and the random-adding methods and present some general aspects of the random-adding method for the simple case of hard core–soft shell objects (or particles). In Sec. IV we extend this method to a more general potential and suggest a "global" characterization of the equilibrium state of interacting systems for the percolation problem. Section V describes the implementation of this generalization into a computer algorithm. In Sec. VI we compare the results of our method with those of the Metropolis method and we show that our approach retains accurately the basic features of the connectivity of percolating systems. Finally, Sec. VII highlights the most important implications of the present work.

II. BACKGROUND

In recent years, continuum percolation [2] has been a field of growing interest. The connectivity and its physical implications in continuum systems of objects (or particles) is of relevance to many fields in physics, ranging from properties of porous media [3] to the physics of microemulsions [4]. In particular, recent interest has concentrated on the physics of systems and processes composed of interacting objects. Conspicuous examples are water [5], molecular liquids [6], microemulsions [4], deposition processes [7], and polymerization [8].

The problem of percolation in systems of interacting objects holds a peculiar place in percolation theory. Historically, percolation theory made its major advances through lattice models [9]. These enable predictions of the universal characteristics of percolation systems, such as critical exponents, which are identical for all lattices and continuum systems (except for the transport proper-

ties). On the other hand, the percolation threshold is system dependent. For continuum systems of permeable objects, considerable theoretical success can be obtained from analogies between continuum systems and lattice systems [10] or from analytical theories [11,12]. On the "experimental" side, computer simulations are a very practical means of finding the percolation threshold of a continuum system of permeable objects [13,14]. However, when it comes to systems of interacting objects, analytical attempts to derive the percolation threshold of continuum systems have met with only limited success [15–17]. Most of the results obtained thus far are only qualitative and show marked quantitative deviations from the results of computer simulations [15]. On the other hand, some success has been obtained for lattice systems [18,19]. Prominent among these is a class of models known as percolation in correlated sequential adsorption [20,21] (CSA), in which adsorption rates on a site in a lattice can be enhanced if neighboring sites are occupied. Like other lattice systems, however, CSA does not relate directly to a physical microscopic interaction, and the enhanced adsorption rates are chosen rather arbitrarily. Moreover, as mentioned above, the percolation threshold is a system dependent property, and therefore lattice systems are unlikely to be very useful representations of continuum systems. In view of the relative failure of analytical methods, the percolation threshold of the continuum system of interacting objects must be determined, at present, through computer simulations. For such systems the only available computer simulation method up to now is the Metropolis method [22,23], which has been used [4] for percolation in connection with models of microemulsions [24]. However, this method is lengthy in its use of a large amount of computer time and it is particularly difficult to apply in percolation problems, because in a Metropolis run, the density remains fixed. Thus, one must make a series of such runs with varying densities in order to find the percolation threshold.

Because of this, the Metropolis procedure is an unnatural and not too efficient way of finding the threshold. Nonetheless, there is no other known way of simulating the equilibrium state of an interacting system, and there seems therefore to be no choice but to use the Metropolis method. In this paper, however, we argue that the connectivity properties of a system (i.e., the percolation threshold) are different from other equilibrium properties, such as the thermodynamic properties or the pair-correlation function, and in principle one may be able to reproduce the percolation threshold of a system without necessarily reproducing all the other equilibrium properties of the system. We prove this assertion by presenting here a simulation method that performs this task. This simulation procedure is different from the Metropolis method but reproduces the percolation thresholds of interacting systems obtained with it. Our method is, however, conceptually simpler as well as more natural and more efficient for percolation problems in general. Its success implies that the connectivity properties of the system *may* depend on fewer details than other equilibrium properties of the system (such as the pair-correlation function). While in this paper we do not concentrate on this general question, we nonetheless think that it is an intriguing line of inquiry that should be pursued further.

III. THE METROPOLIS AND THE RANDOM-ADDING METHODS

As we mentioned in Sec. II, the Metropolis algorithm starts with a given density of objects which remains constant during the whole run. Starting from some initial configuration, new ones are generated by random trial changes, usually a shift in the position of one of the particles in the system. Every such trial change is accepted or rejected according to a criterion based on the change ΔE in the total energy of the system that the trial move produces. There are two cases: (a) If $\Delta E \leq 0$ (hence, the total energy diminishes), the trial change is accepted. (b) If $\Delta E > 0$, a random number s between 0 and 1 is generated. This number is then compared with the Boltzmann factor $\exp(-\beta\Delta E)$ where $\beta = 1/k_B T$, T is the temperature of the system and k_B is Boltzmann's constant. If $s \leq \exp(-\beta\Delta E)$ the trial change is accepted, otherwise it is rejected.

Conditions (a) and (b) ensure that a long series of thusly generated configurations conforms to the Gibbs distribution [23]. Such a series then serves to calculate statistical averages of physical quantities. In percolation problems [4], this algorithm is used to calculate the average probability, P, for the existence of a spanning cluster in the system. The critical density is defined as the one for which P reaches a prechosen value (the authors of Ref. [4] use $P = 0.5$, but the critical density is relatively insensitive to the precise value chosen [4]). Because the Metropolis process cannot, as a practical matter, be implemented with a large number of objects (typically a few hundreds), a large number of Metropolis steps are required to ensure that fluctuations and statistical uncertainties are small (for example, in Ref. [4] about $N = 500$ particles and 4×10^4 steps per particle have been used). For the purpose of computing the percolation thresholds this makes the Metropolis method quite lengthy, even before the density is varied. Furthermore the need for a full run of the simulation for each different object concentration is impractical and somewhat unnatural for percolation. A more natural method would be to increase continuously the objects density and wait for percolation to occur. This is the basis of the random-adding procedure.

This random-adding procedure is commonly used for the case of zero interactions (permeable objects) with bonding defined by partial overlap of the objects [11–13,25–27]. Objects are "thrown" into the system at random locations and the concentration is increased until a spanning duster is obtained. Thanks to an efficient algorithm developed by Hoshen and Kopelman [28], such a simulation [12] can be conveniently carried out with large samples (typically $N \geq 10^4$). In this case, the absence of interactions makes all configurations equally probable. Since the random-adding procedure generates configurations totally at random, it clearly reproduces the equilibrium state of the system. This ceases to be the case when interactions are present. Even for the simplest possible system, that is, a system of hard spheres, it has been

known for some time that the random-adding procedure does not reproduce the equilibrium state [29]. For the case of hard spheres, the random-adding method takes the following form: at each step, one "throws" in a sphere's center at a random location. If the newly added sphere overlaps one of the previously placed spheres, it is removed and a new sphere is thrown in its place. The process is repeated until no more spheres can be accepted to the system. We conclude then that in the random-adding procedure the "history" of the system, i.e., its process of buildup, introduces a statistical bias that makes some configurations *a priori* more probable than others [29]. Hence, the random-adding method produces preferentially a certain type of configuration. This is in contrast with the true equilibrium distribution, where all the allowed configurations (where no overlap of spheres occurs) are equally probable. This *in itself* leaves open the question of whether or not the preferred configurations reproduce the equilibrium state of the system. Not all (equally probable) configurations, after all, represent adequately the equilibrium state of the system. This may be immediately appreciated by simply considering the example of a perfectly ordered configuration in which all the spheres are neatly stacked in one corner of the system. It is basically an "empirical" question whether or not the random-adding generated configuration belongs to the dominant class of true equilibrium configurations. In general, however, the answer is that it does not. For example, Widom [29] has shown by explicit calculations in one-dimensional systems that the thermodynamic properties of the random-adding configuration are different from the true equilibrium ones.

Connectivity, however, is a different property of the system. Therefore, it is not obvious that random-adding generated configurations have percolation thresholds different from those of true equilibrium configurations. The question is most easily answered by a direct check. The authors of Ref. [4], for example, determined the percolation threshold of a system of three-dimensional hard spheres and two-dimensional hard disks (using the Metropolis method, i.e., the equilibrium configuration). In both cases, the binding criterion was provided by adding a "soft shell" of diameter d. Two objects are bound if their shells overlap, that is, if their *centers* are separated by a distance smaller than d. We have used a random-adding procedure with a removal criterion to determine the percolation thresholds of the same systems. As described above, the configuration is generated sequentially by "throwing in" new objects at random locations. If overlap of the hard cores occurs, the last thrown object is removed and another is thrown in its place. This goes on until a spanning cluster appears in the system. The concentration at which this happens, ρ_c, is then the percolation threshold. The sample space volume is usually normalized to unity and the critical concentration is numerically equal to the critical number of objects in the system, N_c. In all our runs, the size of the objects was chosen so that N_c was about 20 000. It is usual [4,12] to eliminate dependence on objects' size by measuring the percolation threshold in dimensionless units. We chose to measure $(4\pi/3)\rho_c d^3$ in the case of a system of spheres and $\pi\rho_c d^2$ in the case of disks. These normalizations were chosen to accord with accepted usage in the limit of zero hard core radius, i.e., permeable objects [11]. In this case it is usual to use the quantity B_c defined as $\rho_c V_{\rm exc}$, where $V_{\rm exc}$ is the excluded volume around every object. In the present case, this corresponds to $(4\pi/3)d^3$ in three dimensions and πd^2 in two. Figures 1(a) and 1(b) present the result of our random-adding method for the case of a system of spheres with a hard core and a system of disks with a hard core, respectively. We compare our results with those obtained by the Metropolis procedure of Ref. [4]. The "hard core" diameter is σ and the "soft shell" diam-

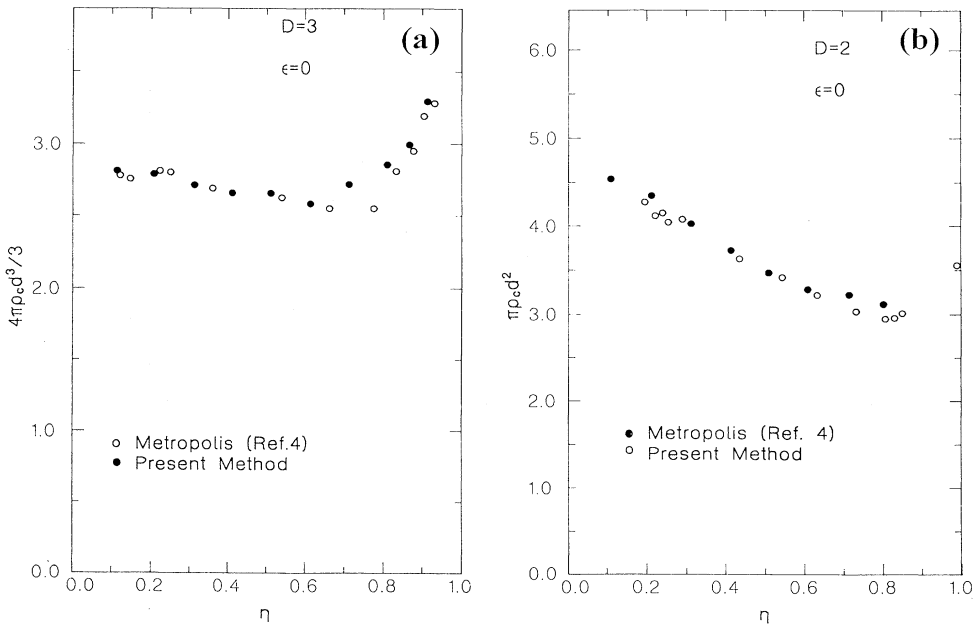

FIG. 1. Percolation thresholds as a function of the ratio η for a system of hard core spheres (a) and for a system of hard core disks (b).

eter is d. The normalized percolation threshold is presented as a function of the ratio of these two quantities, i.e., $\eta=\sigma/d$. This is to facilitate comparison with the results of Ref. [4], which were presented in this form. The physical explanation for the dependence of the threshold on η was given in Ref. [4] and thus will not be repeated here. For the present purpose, what matters is the *striking agreement* between our random-adding results and the Metropolis results. This is an impressive confirmation of the conjecture that random-adding generated configurations have the *same* thresholds as true equilibrium configurations. Moreover, in this case our simple algorithm is very quick, while by comparison, the Metropolis procedure is very inefficient and uses a much larger amount of computer time. It should be noted however that random-adding algorithms exhibit "jamming" above some densities [30], namely, no more objects may be thrown into the system for lack of available space. If jamming occurs, before percolation is reached, the threshold cannot be determined even though it may be well defined. Jamming is another "historical" property of random-adding algorithms and does not necessarily represent a true property of the equilibrium system [29]. Nonetheless, Fig. 1 shows that jamming only occurs at high values of η (specifically at $\eta>0.84$ for disks, and $\eta>0.9$ for spheres), where Metropolis runs are also difficult to perform. For most practical purposes therefore, the random-adding procedure is adequate.

These results show that the "historical bias" introduced into the random-adding procedure by its sequential addition character is unimportant for determining percolation thresholds below the jamming density. This raises the question of whether or not such a procedure can be adapted to other more generic interactions. Such a generic interaction should include an attractive "tail" as well as a short range (hard core type) repulsive term. Let us take the *heuristic* position that *percolation thresholds are insensitive to the historical bias of random-adding algorithms, for all interactions.* We shall have to demonstrate this assertion, but we temporarily adopt it without proof. This leaves the question of the physical effect of the interaction, namely that not all allowed configurations are equally probable even in *true equilibrium.* We shall show presently that this can be taken into account by modifying and extending the removal criterion. To be specific, we shall work with the square-well potential model used by the authors of Ref. [4]. Before we can describe the actual computer simulation procedure, however, we need to derive a criterion for the equilibrium configuration of the interacting system. According to our heuristic principle, we shall then assume that this criterion can be applied to the random-adding algorithm without further concern for the sequential "historical bias."

IV. DEVELOPMENT OF THE REJECTION CRITERION FOR THERMAL EQUILIBRIUM

In Ref. [1] we have suggested a rejection criterion based on the simple picture of a central-particle potential neglecting the many particle interactions to which the particles are subjected. Here, we systematically derive the criterion which justifies the heuristic approach taken in Ref. [1].

We consider a system of $N+1$ spherical particles, with an interparticle interaction that consists of an infinitely repulsive hard core of diameter σ and a square-well attractive term of range $\sigma(1+\lambda)$, where λ is a fixed parameter. The interaction potential $u(r)$ between two particles, the centers of which are a distance $r(=|\mathbf{r}|)$ apart, is given by

$$u(r)=\begin{cases}\infty\ , & r<\sigma\\ -(k_BT)\epsilon\ , & \sigma<r<\sigma(1+\lambda)\\ 0\ , & \sigma(1+\lambda)<r\ ,\end{cases} \tag{1}$$

where T is the temperature, k_B is Boltzmann's constant, and ϵ is a parameter that defines the attractive interaction's strength. This is the potential used by the authors of Ref. [4]. Clearly, because of the interaction the particles are not distributed randomly in the system. We seek then a characterization of the distribution of particles in the system at thermal equilibrium. To find it, we select an arbitrary particle, denoted hereafter as particle 0, and consider how the remaining N particles are distributed around it. We expect that the attractive interaction will cause a clustering of particles around particle 0. More formally, let $\rho(r)$ be the local particle density at a distance r from particle 0. Because of the attractive interaction, we expect that $\rho(r)$ will be greater, on average, in the range $\sigma<r<\sigma(1+\lambda)$ than in the range $r>\sigma(1+\lambda)$. We calculate this effect by determining how many particles will fall in the range $\sigma<r<\sigma(1+\lambda)$, on average.

To this end, we calculate the probability of finding k particles at positions $\mathbf{r}_1,\mathbf{r}_2,\ldots,\mathbf{r}_k$, all within the attractive interaction range, that is, such that $\sigma<|\mathbf{r}_j|<\sigma(1+\lambda)$ for $j=1,2,\ldots,k$. The probability of finding N particles at positions $\mathbf{r}_1,\ldots,\mathbf{r}_N$ relative to particle 0 is given in the canonical ensemble [31] by

$$P(1,\ldots,N)=(1/Q_N)\exp[-\beta H(1,\ldots,N)]\ , \tag{2}$$

where $\beta=1/k_BT$, H is the system's Hamiltonian, and Q_N is the configuration integral, defined [31] as

$$Q_N=\int d1\ldots dN\exp[-\beta H(1,\ldots,N)]\ , \tag{3}$$

where all the integrations are performed over the entire volume of the system, denoted Ω.

The probability of finding k particles at positions $r_1,\ldots,r_k$ within the interaction range of particle 0, so that all remaining particles are outside this range, is now

$$P(1,2,\ldots,k)=\begin{bmatrix}N\\ k\end{bmatrix}\int d(k+1)\ldots dN\,P(1,\ldots,N)\ , \tag{4}$$

where the combinatorial factor $\binom{N}{k}$ is the number of ways of selecting k particles out of N, and all the integrations are performed over the positions *outside* the interaction range of particle 0. We now break up the Hamiltonian into four parts in the following way:

$$H(1,\ldots,k,k+1,\ldots,N)=E(1,\ldots,k)+W(1,\ldots,k)+\phi_k(k+1,\ldots,N)+V(k+1,\ldots,N)\ ,$$

where

$$\begin{aligned} E(1,\ldots,k)&=\sum_{i=1}^{k}u(0,i)\ ,\\ W(1,\ldots,k)&=\sum_{\substack{i>j\\ j=1}}^{k}u(i,j)\ ,\\ \phi_k(k+1,\ldots,N)&=\sum_{j=k+1}^{N}\left[\sum_{i=1}^{k}u(i,j)\right]\ ,\\ V(k+1,\ldots,N)&=\sum_{\substack{i>j\\ j=k+1}}^{N}u(i,j)\ . \end{aligned} \tag{5}$$

Physically, E is the interaction energy of the k particles $1,2,\ldots,k$ with particle 0. W is the mutual interaction energy of these k particles among themselves. ϕ_k is the interaction energy of the other $N-k$ particles, denoted $k+1,\ldots,N$, with the above k particles $1,\ldots,k$. Finally, V is the mutual interaction energy of the $N-k$ particles $k+1,\ldots,N$ among themselves. We note that since $\sigma<|\mathbf{r}_j|<\sigma(1+\lambda)$ for $j=1,2,\ldots,k$, we have that

$$E(1,\ldots,k)=-k\epsilon/\beta\ . \tag{6}$$

We introduce two notations: the volume of the attractive well around particle 0 is denoted V_b, while the volume outside this range is V_o. Thus, in three dimensions

$$\begin{aligned} V_b&=(4\pi/3)\{[\sigma(1+\lambda)]^3-\sigma^3\}\ ,\\ V_o&=\Omega-(4\pi/3)[\sigma(1+\lambda)]^3\ , \end{aligned} \tag{7a}$$

and in two dimensions

$$\begin{aligned} V_b&=\pi\{[\sigma(1+\lambda)]^2-\sigma^2\}\ ,\\ V_o&=\Omega-\pi[\sigma(1+\lambda)]^2\ . \end{aligned} \tag{7b}$$

Using Eq. (6), we rewrite Eq. (4) in the following form:

$$P(1,\ldots,k)=\binom{N}{k}(1/Q_N)\exp[k\epsilon-\beta W(1,\ldots,k)]\times\int d(k+1)\cdots dN\exp[-\beta(\phi_k+V)]\ , \tag{8}$$

where all integrations are performed over the volume V_o defined in Eqs. (7). We concentrate on the integral on the right-hand side of Eq. (8), i.e., on

$$Q_{N-k}=\int d(k+1)\cdots dN\exp[-\beta(\phi_k+V)]\ . \tag{9}$$

Comparison with Eq. (3) shows that this is the configuration integral of a system of volume V_o containing $N-k$ particles which mutually interact via an internal potential V and subject to an exterior field ϕ_k that depends on k external parameters, $\mathbf{r}_1,\ldots,\mathbf{r}_k$. The field ϕ_k, however, is short ranged, as is obvious from its definition [Eqs. (5)]. It acts only near the surface of the volume V_o, that is, near the surface $|\mathbf{r}|=\sigma(1+\lambda)$. In the thermodynamic limit, such surface terms are negligible [32]. Therefore, we can safely approximate Eq. (9) as

$$Q_{N-k}=\int d(k+1)\cdots dN\exp(-\beta V) \tag{10}$$

which is exact in the thermodynamic limit. In this limit, we can define the reduced configuration integral, q, as

$$q=\lim_{\substack{N\to\infty\\ \Omega\to\infty}}(Q_N/\Omega^N)\ . \tag{11}$$

The reduced configuration integral is independent of Ω and N. It depends only on the density of the particles, ρ, the temperature, and the details of the microscopic interaction [32]. These parameters are identical for the original system of volume Ω and for the system of $N-k$ particles in the volume V_o. Therefore, we have that

$$Q_{N-k}=qV_o^{N-k}\ . \tag{12}$$

Hence,

$$Q_{N-k}/Q_N=(V_o/\Omega)^N V_o^{-k}\ . \tag{13}$$

Using Eq. (13) and writing $\binom{N}{k}$ explicitly as $N(N-1)\cdots(N-k+1)/k!$ and approximating it as $N^k/k!$, we can finally recast Eq. (8) in the form

$$P(1,\ldots,k)=P(0)[N\exp(\epsilon)/V_o]^k(1/k!)\times\exp[-\beta W(1,\ldots,k)]\ , \tag{14}$$

where $P(0)\equiv(V_o/\Omega)^N$.

The probability $P(k)$ of finding exactly k particles anywhere in the range V_b is now

$$P(k)=\int_{V_b}d1\cdots dk\,P(1,\ldots,k)\ . \tag{15}$$

We introduce now the following notations:

$$T_k\equiv(1/V_b)^k\int_{V_b}d1\cdots dk\exp[-\beta W(1,\ldots,k)]$$

and

$$\Delta\equiv\rho\exp(\epsilon)V_b\ , \tag{16}$$

where ρ is the average density of the particles in the system. We define $T_0\equiv1$. Since $(N/V_o)=\rho$ for large N, Eq. (15) becomes

$$P(k)=[P(0)/k!]\Delta^k T_k\ . \tag{17}$$

The average number of particles in the range V_b, $\langle k\rangle$, is now given by

$$\langle k\rangle=\sum_{k=0}^{\infty}kP(k)/\sum_{k=0}^{\infty}P(k)\ . \tag{18}$$

This result is more suggestive when expressed through the ratio of the following two densities: $\langle k\rangle/V_b$, which we denote ρ_b, is the average density of particles within the interaction range (V_b) of particle 0. $(N-\langle k\rangle)/V_o$, which we denote ρ_o, is the average density of particles outside the interaction range of particle 0. Simple algebra and use of the definition of Δ [Eq. (16)] then yields that

$$\rho_o/\rho_b = A\exp(-\epsilon)\ , \tag{19}$$

where $A=[1+\Delta T_1+(\Delta^2/2!)T_2+\cdots]/[T_1+\Delta T_2+(\Delta^2/2!)T_3+\cdots]$.

Equation (19) can be checked for a particular physical situation. Let us assume that $W(1,\ldots,k)=0$ in Eq. (5). This means that the system is an ideal gas subject only to the field of particle 0; while this is not a realizable physical situation, it is a convenient check of Eq. (19). In this case, we have that $T_i=1$ for all i's, and therefore $A=1$. Hence in this case $\rho_o/\rho_b=\exp(-\epsilon)$, which corresponds to the Boltzmann distribution for an ideal gas subjected to an external force field [32] (here originating in particle 0). It is now remarkable that A is in fact not markedly different from 1, even when the mutual energy interaction $W(1,\ldots,k)$ is correctly taken into account. A precise calculation of A is quite difficult to carry out, but as we show presently, it is also unnecessary. We define an "A series" as follows:

$$A_1=(1+\Delta T_1)/T_1\ ,$$

$$A_2=(1+\Delta T_1+0.5\Delta^2 T_2)/(T_1+\Delta T_2)\ ,$$

$$A_j=\frac{1+\Delta T_1+\cdots+(\Delta^j/j!)T_j}{T_1+\Delta T_2+,\cdots,+[\Delta^{j-1}/(j-1)!]T_j}\ . \tag{20}$$

Every term A_j is defined by the j quantities $T_1,\ldots,T_j$. In the limit $j\to\infty$, A_j approaches A. To evaluate this limit we calculate the first terms in the $\{A_j\}$ series and use the Shanks-Wynn ϵ algorithm extrapolation scheme [33] to approximate the contribution of the remaining terms. The term T_1 is trivial, since obviously $W=0$, there being only one particle in the volume V_b. Thus $T_1=1$. T_2 is slightly more complicated and the details can be found in Appendix A. The final result is given by

$$T_2=1-a+bf\ , \tag{21}$$

where $a=(1/V_b^2)[I_3-2I_2+I_1]$, $b=(1/V_b^2)[I_4-3I_3+3I_2-I_1]$, the I_j's refer to the integrals in Table I, and $f\equiv\exp(\epsilon)$.

Equation (21) can be given a simple geometric interpretation which we present in Fig. 2. In this figure we have depicted particle 0 and particle 1. Particle 2 is not shown, but it can now be positioned only in the shaded or in the cross-hatched areas, if it is to fall in the interaction range of particle 0, as required for T_2. In the shaded area $\exp[-\beta u(1,2)]=1$, while in the cross-hatched area $\exp[-\beta u(1,2)]=f$ [according to Eq. (A3)]. The interpretation of Eq. (21) is now immediate: the shaded area is $V_b(1-a)$ and the cross-hatched area is $V_b b$. This can be confirmed by a direct calculation of the corresponding areas. We note that aV_b is the area "cut out" from V_b by the total interaction range of particle 1 [the interaction range is a sphere or disk of radius $\sigma(1+\lambda)$]. This geometric interpretation is important for the evaluations of T_3. The integrals defining T_3 are notoriously difficult to calculate analytically [34]. However, for small values of λ (thin interaction shells), the above geometric arguments can provide a very good evaluation. Fortunately, the authors of Ref. [4] used $\lambda=0.1$. Since we are interested ultimately in comparing our random-adding results with the Metropolis results of Ref. [4], we need only evaluate T_3 for the $\lambda=0.1$ case. Our geometric method is expected to yield the correct T_3 value to within 10%. This turns out to be quite sufficient for our purpose (see

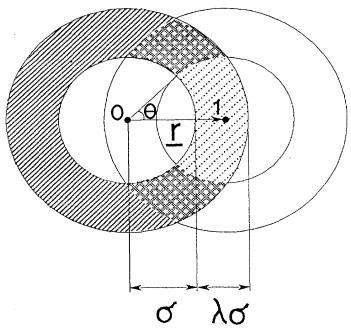

FIG. 2. The configuration of particles corresponding to the term T_2. Only particles 0 and 1 are depicted. Particle 3 may be located either in the shaded or in the cross-hatched areas.

TABLE I. The integrals needed to calculate T_2 [Eq. (21)].

Three dimensions

$$I_1=(5\pi^2/6)\sigma^6$$

$$I_2=\begin{cases}(16\pi^2/9)\sigma_6 & \text{if } 1+\lambda>2\\ \pi^2\sigma^6[\frac{16}{9}(1+\lambda)^3-(1+\lambda)^4+\frac{1}{18}(1+\lambda)^6] & \text{otherwise}\end{cases}$$

$$I_3=\pi^2\sigma^6[\tfrac{16}{9}(1+\lambda)^3-(1+\lambda)^2+\tfrac{1}{18}]$$

$$I_4=(5\pi^2/6)(1+\lambda)^6\sigma^6$$

Two dimensions

$$I_1=(\pi-3\sqrt{3}/4)\pi\sigma^4$$

$$I_2=\begin{cases}\pi^2\sigma^4 & \text{if } 1+\lambda>2\\ \sigma^4\{\pi^2(1+\lambda)^2-(\pi/4)[(1+\lambda)^3+2(1+\lambda)]\sqrt{4-(1+\lambda^2)}+2\pi[1-(1+\lambda)^2]\arcsin[(1+\lambda)/2]\} & \text{otherwise}\end{cases}$$

$$I_3=\sigma^4\{\pi^2(1+\lambda)^2-(\pi/4)[1+2(1+\lambda)^2]\sqrt{4(1+\lambda)^2-1}+2\pi(1+\lambda)^2[(1+\lambda)^2-1]\arcsin[2/(1+\lambda)]\}$$

$$I_4=(\pi-3\sqrt{3}/4)\pi\sigma^4(1+\lambda)^4$$

Sec. V). The detailed arguments for the calculation of T_3 are presented in Appendix B. Here we merely quote the final results:

$$T_3=1-3a+2.25a^2+0.5(ab-b^2)$$
$$+f[3b-4.5ab+0.75b^2]+f^2[1.25b^2] . \quad (22)$$

Hence, for the case $\lambda=0.1$ we can sum up the results, using Eqs. (21) and (22) and Table I. We obtain then that in two dimensions

$$T_1=1 ,$$
$$T_2=0.684+0.035f , \quad (23a)$$
$$T_3=0.258+0.056f+0.0015f^2 ,$$

and in three dimensions

$$T_1=1 ,$$
$$T_2=0.774+0.048f , \quad (23b)$$
$$T_3=0.441+0.096f+0.0028f^2 .$$

This allows us to calculate the terms A_1, A_2, A_3 in the series defined in Eq. (20). Using the ϵ algorithm, we can obtain an estimate for the limit of the series, hereafter denoted by A_ϵ. This estimate is given [33] by

$$A_\epsilon=A_2+[(A_2-A_1)(A_3-A_2)/(2A_2-A_1-A_3)] . \quad (24)$$

The behavior of A_ϵ as a function of the parameter Δ is presented in Fig. 3(a) for two dimensions with $\epsilon=2.0$, and in Fig. 3(b) for three dimensions with $\epsilon=2.08$ (these values for ϵ were used by the authors of Ref. [4]). The figures show that A_ϵ varies quite slowly with Δ, and remains fairly close to 1. We note that from Eqs. (16) and (19) it follows that $\Delta\simeq A\rho_b V_b$ (since $\rho\simeq\rho_o$). Because $\rho_b V_b$ is the average number of particles in the interaction shell of particle 0, Δ must be of the order of unity. Thus, as shown by Fig. 3, for such values of Δ, A_ϵ remains quite close to 1. Equation (19) can now be approximated by

$$\rho_o/\rho_b=A_\epsilon\exp(-\epsilon) . \quad (25)$$

Equation (25) is the equilibrium criterion we use in our computer simulation. Basically, our algorithm removes newly added particles if hard core overlap occurs *or* if Eq. (25) is violated. We now describe its implementation.

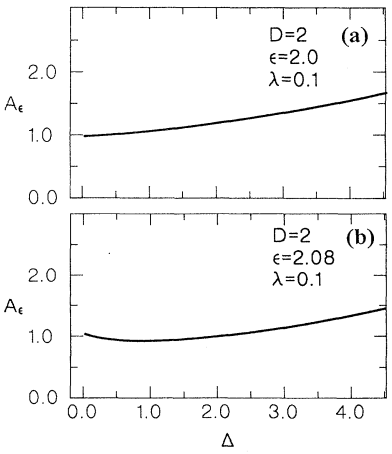

FIG. 3. The dependence of A_ϵ on the parameter Δ for a two-dimensional system of disks with $\epsilon=2.0$ and $\lambda=0.1$ (a), and for a three-dimensional system of spheres with $\epsilon=2.08$ and $\lambda=0.1$ (b).

V. THE RANDOM-ADDING SIMULATION ALGORITHM

Following the development of the rather general criterion we are in a position to apply it to actual simulations for the determination of the percolation threshold. For this purpose we define the following quantities:

$$N_b=\text{average number of particles such that } \sigma<r<\sigma(1+\lambda) ,$$
$$N_o=\text{average number of particles such that } r>\sigma(1+\lambda) , \quad (26)$$

where in both cases r is the distance between the particles in question and particle 0. Therefore, we have that

$$\rho_b=N_b/V_b ,$$
$$\rho_o=N_o/V_o . \quad (27)$$

We cannot require, however, that Eq. (25) be verified as such, since the probability of obtaining an exact equality is negligible. We must therefore require an inequality, i.e.,

$$\rho_o/\rho_b\le A_\epsilon\exp(-\epsilon) . \quad (28)$$

The reason we chose this particular inequality rather than the reverse $\ge$ sign is as follows: Consider the alternative to Eq. (28), namely $\rho_o/\rho_b\ge A_\epsilon\exp(-\epsilon)$. This is an *upper bound* on ρ_b of the form $\rho_b\le\rho_o\exp(\epsilon)A_\epsilon$. Now, our algorithm works by random addition. Thus, left to itself, it tends to produce values of ρ_o/ρ_b quite close to 1. As a result, if ϵ is large enough, the upper bound on ρ_b is always satisfied by a simple hard core random-adding algorithm. This, however, produces result adequate for $\epsilon=0$, but not for large ϵ's. Thus, the upper bound does not represent an adequate restriction on the algorithm's workings. Equation (28), on the other hand, is a *lower bound* on ρ_b and as such should produce the expected rise in ρ_b as the interaction (the parameter ϵ) is increased.

Our algorithm proceeds as follows: First a "particle" is thrown into the system and a second one is added in such a way that it falls within the first one's attractive shell. This is to ensure that N_b is not zero, since otherwise, Eq. (28) is violated and the particle is always rejected.

At each step, a new particle is randomly thrown into the system and the total number of particles (a counter I) is increased by 1. The program then makes two sweeps of the sample and checks several criteria. In the first

sweep, the algorithm checks whether the new particle's hard core overlaps the hard core of any other particle. This step is made more efficient by dividing the sample space into subregions and checking only subregions where intersection is possible [12]. If such an overlap occurs the particle is removed, I is decreased by one, and a new particle is thrown in. If after the first sweep, the particle is (temporarily) accepted, a second sweep is made in which the algorithm checks the distance r between the new object and all other (previously thrown in) objects. For each such pair, if $\sigma < r < \sigma(1+\lambda)$, a counter K is incremented by 1. The averages N_b and N_o [Eq. (26)] are calculated recursively in the following way:

$$N_b = [(I-1)N_b(\text{previous}) + K]/I \ ,$$
$$N_o = [(I-1)N_o(\text{previous}) + I - 1 - K]/I \ . \tag{29}$$

These expressions are recursive equivalent to calculating N_b and N_o by the expressions

$$N_b = \sum_{j=1}^{N} n_j / I \ ,$$
$$N_o = \sum_{j=1}^{N} (I - 1 - n_j)/I \ , \tag{30}$$

where n_j is the number of particles located within the attractive shell of particle j. Equations (30) are clearly equivalent to Eqs. (26), and therefore, so are Eqs. (29). After completing the second sweep, the algorithm calculates Δ anew by

$$\Delta = IV_b \exp(\epsilon)/\Omega \ , \tag{31}$$

where Ω is the volume of the sample space.

The program then calculates A_ϵ according to Eqs. (20), (23), and (24). Hence, A_ϵ assumes a *different value* after each successful throw, because the density changes and therefore Δ changes. Note that T_1, T_2, T_3 depend only on ϵ and λ and are therefore fixed during the entire run. Finally, one should note that A_ϵ does not depend on the parameter η, i.e., on the binding criterion. This is as it should be, since A_ϵ only characterizes the *interactions* in the system, independently of whether any connectivity property is present or not. The implementation of the criterion, given by Eq. (28), now takes the following form: if $(N_o/V_o)/(N_b/V_b) > A_\epsilon \exp(-\epsilon)$, the new particle is rejected, I is reduced by 1, N_b and N_o are returned to their previous values, and a new particle is thrown in; if not, the new particle is accepted. Each time a newly added particle is accepted, the program checks for the onset of percolation. This is done by a continuum version [12,13] of the Hoshen-Kopelman [28] algorithm. The I value at which this onset takes place is the critical number of particles, N_c, and the threshold is $\rho_c = N_c/\Omega$.

VI. RESULTS OF THE SIMULATIONS FOR $\epsilon > 0$

We have compared our random-adding generated results with the Metropolis results of Ref. [4]. Hence we used the same parameters as those used there, i.e., in Eq. (1) we took $\lambda = 0.1$, and varied ϵ. All the percolation thresholds were measured as in the $\epsilon = 0$ case (Fig. 1), i.e., $(4\pi/3)\rho_c d^3$ in three dimensions and $\pi\rho_c d^2$ in two dimensions. As in Ref. [4], these quantities are plotted as a function of the ratio $\eta = \sigma/d$ where σ is the hard core diameter and d the soft shell diameter. Two particles are bound if their centers are distant by less than d. In all our runs, N_c was between 10 000 and 15 000. Every result plotted in the figures is the average of five independent runs performed with the same parameters every time. The statistical variations between the five runs were up to 15%. While this may seem a rather large variation, the average over five runs is quite stable, in the sense that when we made ten runs of the program, for a few cases, the average over ten runs differed from the average over five runs by only about 5%, with a maximum deviation of 10%.

The results for three dimensions and $\epsilon = 2.08$ are presented in Fig. 4, and those for two dimensions and $\epsilon = 2.0$ in Fig. 5. The agreement with the Metropolis results is excellent. The slight discrepancies between our results and those of Ref. [4] are not greater than between different runs of simulations of identical systems with identical methods. In all these systems we note that, as in the $\epsilon = 0$ case, jamming occurs only at high values of η. The situation is different for higher values of ϵ. Figure 6 presents our results for $\epsilon = 2.86$ in two dimensions. Here jamming occurs very early on (at $\eta \geq 0.3$) and we could not obtain results for higher values of ϵ. Nonetheless the behavior of the threshold for small η follows the trend of the Metropolis method. We checked this tendency by reducing ϵ until jamming occurred at sufficiently high values of η to exhibit the detailed behavior of the threshold. We found that a value of $\epsilon = 2.2$ fulfills this require-

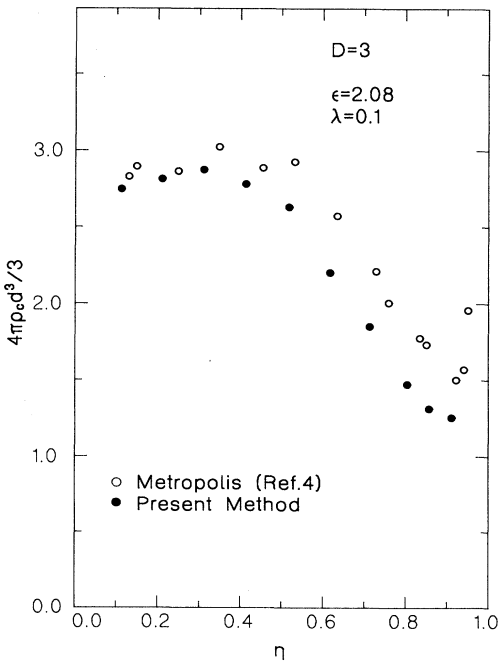

FIG. 4. Percolation thresholds as a function of the ratio η for a three-dimensional system of spheres with $\epsilon = 2.08$ and $\lambda = 0.1$.

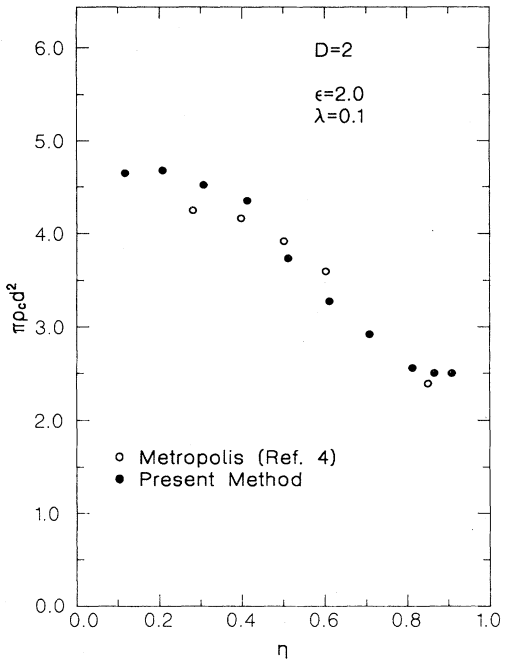

FIG. 5. Percolation thresholds as a function of the ratio η for a two-dimensional system of disks with $\epsilon=2.00$ and $\lambda=0.1$.

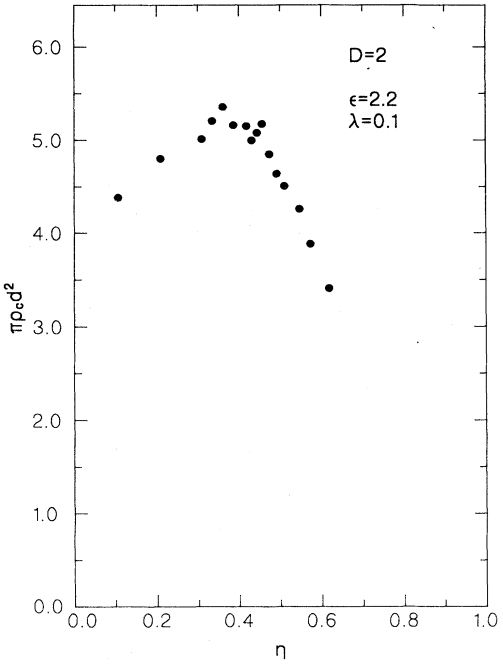

FIG. 7. Percolation thresholds as a function of the ratio η for a two-dimensional system of disks with $\epsilon=2.2$ and $\lambda=0.1$.

ment in two dimensions. The results obtained for this case are shown in Fig. 7. In this case we had no Metropolis results to compare our results to, but the *qualitative* dependence of the threshold on the parameter η is strikingly similar to the one exhibited by the Metropolis results for $\epsilon=2.86$ (Fig. 6). This behavior is far from trivial and accidental agreement is excluded. Clearly, as long as we are below the jamming density, our random-adding algorithm reproduces faithfully the Metropolis results.

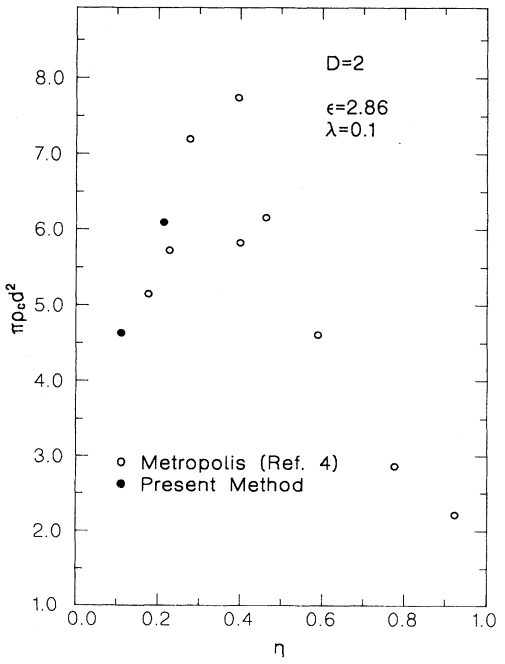

FIG. 6. Percolation thresholds as a function of the ratio η for a two-dimensional system of disks with $\epsilon=2.86$ and $\lambda=0.1$.

Finally, we checked the sensitivity of our method to the value of A_ϵ in the criterion given by Eq. (28). Since we could only *evaluate* the correct value of A, it is important to assess how A dependent the method is. As we showed in Fig. 3, A itself does not change much from unity. Thus it would appear that its exact value is not very important. We verified this conjecture by running our random-adding algorithm with $A_\epsilon=1$ in criterion (28). Indeed the comparison made in Figs. 8(a) and 8(b) shows that the results obtained with $A_\epsilon=1$ and with the correct criterion [Eq. (28)] are remarkably consistent. This verifies our conjecture that the method is insensitive to the precise value of A_ϵ and gives *a posteriori* justification to the approximations used in calculating T_3 (see Appendix B).

VII. CONCLUSIONS

We have presented a random-adding algorithm that reproduces the percolation thresholds of interacting systems (under the jamming density). This is in spite of the known fact that other statistical equilibrium properties of the system are *not* correctly reproduced by random-adding algorithms even for the $\epsilon=0$ case. This points to an intriguing aspect of connectivity that sets it apart from other equilibrium properties. Clearly, the class of configurations which share the same connectivity property is larger than the class of equilibrium configuration. This could be because connectivity is less sensitive to the details of the configurations or for some other reason unknown to us. We did not address here the question of

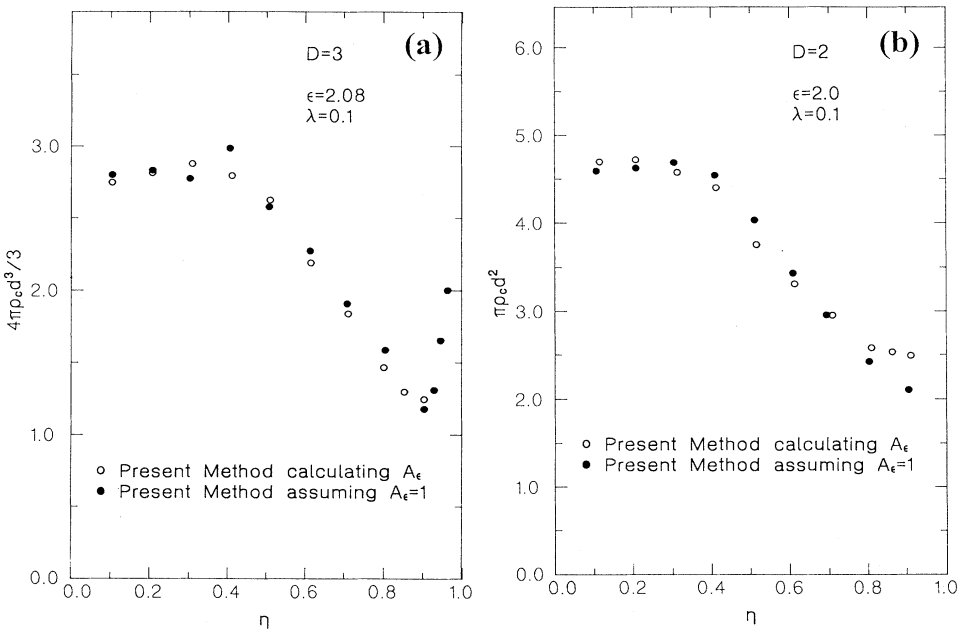

FIG. 8. Comparison of the random-adding generated percolation thresholds with the calculated A_ϵ prefactor and with $A_\epsilon=1$, for (a) spheres with $\epsilon=2.08$ and $\lambda=0.1$, and for (b) disks with $\epsilon=2.0$ and $\lambda=0.1$.

what makes connectivity a "more general" property, in some sense, than other equilibrium properties. Our work does show however that this is certainly the case. The elucidation of this aspect of connectivity could deepen our understanding of this property.

From the more practical point of view, we have shown that the random-adding algorithm can be routinely used for simulations of percolation systems at equilibrium where interparticle interactions take place. The insensitivity of the results to the prefactor which describes the deviation from the single particle central potential model, $[A(\epsilon)]$, to the details of the multiple particle interactions indicates that the present simulation method can be used for getting good estimates of the percolation threshold. This applies even for complicated equilibrium systems for which it is difficult to calculate the above prefactor.

APPENDIX A

We wish to calculate the quantity

$$T_2=(1/V_b^2)\int_{V_b} d1\,d2\,\exp[-\beta u(1,2)]\ . \tag{A1}$$

We define the two functions

$$F_1(\mathbf{r})=\begin{cases}1\ , & |\mathbf{r}|<\sigma\\ 0\ , & |\mathbf{r}|>\sigma\ ,\end{cases}$$
$$F_2(\mathbf{r})=\begin{cases}1\ , & |\mathbf{r}|<\sigma(1+\lambda)\\ 0\ , & |\mathbf{r}|>\sigma(1+\lambda)\ .\end{cases} \tag{A2}$$

From Eq. (1) we have that

$$\exp[-\beta u(\mathbf{r})]=1-(1+f)F_1(\mathbf{r})+fF_2(\mathbf{r})\ , \tag{A3}$$

where $f\equiv\exp(\epsilon)$. Accordingly, T_2 is given now by

$$T_2=(1/V_b^2)\int_{V_b} d\mathbf{x}\int_{V_b} d\mathbf{y}[1-(1+f)F_1(\mathbf{x}-\mathbf{y}) +fF_2(\mathbf{x}-\mathbf{y})]\ . \tag{A4}$$

We can now extend the integrations over the entire system volume Ω, by noting that

$$F_2(\mathbf{r})-F_1(\mathbf{r})=\begin{cases}0\ , & |\mathbf{r}|<\sigma\\ 1\ , & \sigma<|\mathbf{r}|<\sigma(1+\lambda)\\ 0\ , & \sigma(1+\lambda)<|\mathbf{r}|\ .\end{cases} \tag{A5}$$

Consequently, we have that

$$T_2=(1/V_b^2)\int_{\Omega} d\mathbf{x}\int_{\Omega} d\mathbf{y}[F_2(\mathbf{x})-F_1(\mathbf{x})][F_2(\mathbf{y})-F_1(\mathbf{y})] \times[1-(1+f)F_1(\mathbf{x}-\mathbf{y})+fF_2(\mathbf{x}-\mathbf{y})]\ , \tag{A6}$$

where the integration range is defined by the two F_2-F_1 functions. T_2 is now a sum of integrals of the form $\int F_i(\mathbf{x})F_j(\mathbf{y})F_k(\mathbf{x}-\mathbf{y})d\mathbf{x}\,d\mathbf{y}$ where i,j,k only take the values 1 or 2. By suitable changes of the integration variables, all these integrals can be reduced to the form $\int[\int d\mathbf{x}\,F_i(\mathbf{x})F_i(\mathbf{x}-\mathbf{y})]F_j(\mathbf{y})d\mathbf{y}$.

Kirkwood [35] calculated the integral $\int d\mathbf{x}\,F_i(\mathbf{x})F_i(\mathbf{x}-\mathbf{y})$ in 1935. His result for three dimensions is

$$\int d\mathbf{x}\,F_1(\mathbf{x})F_1(\mathbf{x}-\mathbf{y})=\begin{cases}(4\pi\sigma^3/3)[1-(3y/4\sigma)+\frac{1}{16}(y/\sigma)^3]\ , & |\mathbf{y}|\le 2\sigma\\ 0\ , & |\mathbf{y}|>2\sigma\ .\end{cases} \tag{A7}$$

The corresponding expression for $\int d\mathbf{x}F_2(\mathbf{x})F_2(\mathbf{x}-\mathbf{y})$ is obtained from Eq. (A7) by replacing everywhere σ with $\sigma(1+\lambda)$. Similarly, for two dimensions, we found

$$\int F_1(\mathbf{x})F_1(\mathbf{x}-\mathbf{y})d\mathbf{x}=\begin{cases}\pi\sigma^2-(y/2)\sqrt{4\sigma^2-y^2}-2\sigma^2\arcsin(y/2\sigma)\ , & |\mathbf{y}|\le 2\sigma \\ 0\ , & |\mathbf{y}|>2\sigma\ .\end{cases} \tag{A8}$$

All the integrals necessary for calculating T_2 are easily evaluated with the help of Eq. (A7) and Eq. (A8). The results are summarized in Table I. The final result for T_2 is

$$T_2=1-a+bf\ , \tag{A9}$$

where $a=(1/V_b^2)[I_3-2I_2+I_1]$, $b=(1/V_b^2)[I_4-3I_3+3I_2-I_1]$ and the I_j's refer to the integrals in Table I.

APPENDIX B

In this appendix we present the geometric arguments used to calculate T_3, given in Eq. (16), i.e.,

$$T_3=(1/V_b^3)\int\int\int d1d2d3\exp\{-\beta[u(1,2)+u(1,3)+u(2,3)]\}\ . \tag{B1}$$

The geometric interpretation of T_2 for two dimensions is presented in Fig. 2, which shows that $T_2=1-a+bf$ [see Eq. (21)]. The figure depicts only particles 0 and 1. Particle 2 may "sit" in the shaded area [where $\beta u(1,2)=0$] or the cross-hatched area [where $\beta u(1,2)=-\epsilon$]. The angle θ in the figure is given by

$$\cos(\theta)=|\mathbf{r}_1/2|/\sigma\ , \tag{B2}$$

where $\mathbf{r}_1$ is the position of particle 1's center relative to particle 0. Now $\sigma\le|r_1|\le\sigma(1+\lambda)$. For small λ's, the average of $\cos(\theta)$ is given by

$$\langle\cos(\theta)\rangle\simeq\tfrac{1}{2}+\lambda/4\ . \tag{B3}$$

Hence, for $\lambda=0.1$, $\langle\theta\rangle\simeq 0.324\pi$. The exact value of $\langle\theta\rangle$ is $\pi(a-b)$. The dotted area is $\langle\theta\rangle V_b/\pi$. Similarly, the average cross-hatched area is bV_b. For three dimensions, the interpretation is similar.

We can now calculate T_3 according to four different configurations of particles 0, 1, 2, and 3. Once again we work in two dimensions, for the sake of simplicity. Figures 9(a)–9(d) present the four configurations required to calculate T_3. In all the cases, we have depicted particles 0, 1, and 2. Particle 3 may then be placed in either the shaded, cross-hatched, or black areas. The other areas are forbidden because of excluded volume effects. We define now the following function:

$$F(1,2,3)=\exp[-\beta u(1,2)-\beta u(1,3)-\beta u(2,3)]\ . \tag{B4}$$

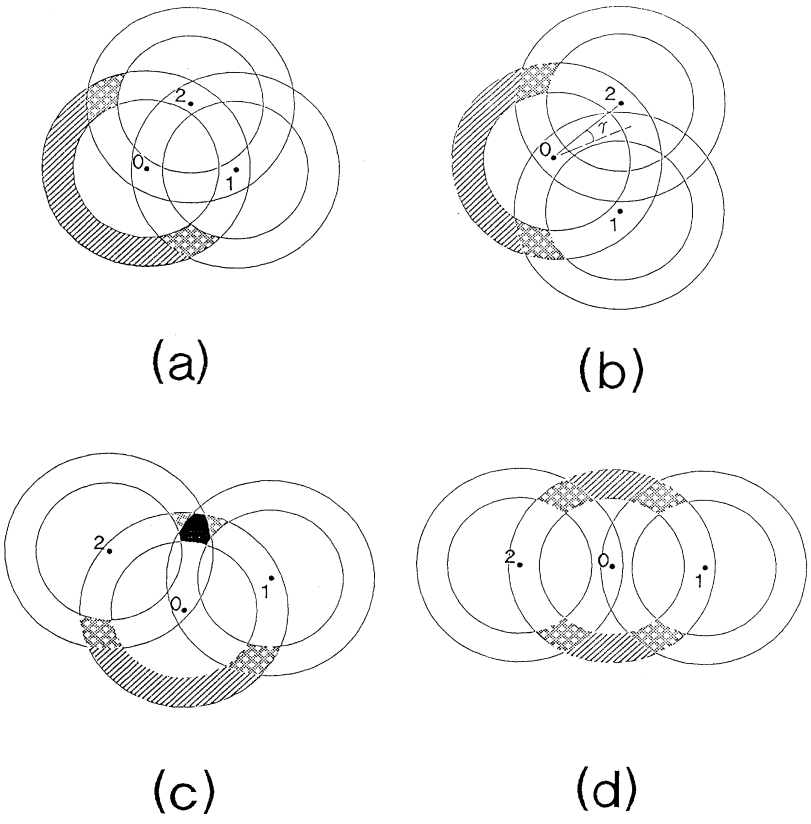

FIG. 9. The various configurations that contribute to T_3. Only particles 0,1,2 are depicted. Particle 3 may only be placed in the shaded, cross-hatched, or black areas.

Let us now consider the four possible configurations one by one:

Case 1: Fig. 9(a). In this case $\beta u(1,2)=-\epsilon$. Hence $F(1,2,3)=f\exp[-\beta u(1,3)-\beta u(2,3)]$, where $f=\exp(\epsilon)$. If particle 3 falls in the shaded area $F(1,2,3)=f$, and if it is in the crosshatched area $F(1,2,3)=f^2$. By arguments similar to those applied for T_2 [see Eq. (A3)], the *average* shaded areas is $(1-3a/2+b/2)V_b$. The cross-hatched area is bV_b. Finally, since $\beta u(1,2)=-\epsilon$, particle 2 must fall in the interaction shell of particle 1. Comparison with Fig. 2 shows that the average area available for such a configuration is bV_b. The total contribution of this configuration T_3 is therefore

$$(T_3)_1=b[(1-3a/2+b/2)f+bf^2]\ . \tag{B5}$$

Case 2: Fig. 9(b). In this case $\beta u(1,2)=0$, hence $F(1,2,3)=\exp[-\beta u(1,3)-\beta u(2,3)]$. If particle 3 falls in the shaded area, $F(1,2,3)=1$; if it falls in the cross-hatched area $F(1,2,3)=f$. The angle γ in the figure is, to a first approximation, in the range $0\le\gamma\le\langle\theta\rangle$, where $\langle\theta\rangle$ is defined by Eq. (B3), and is equal to $\pi(a-b)$ as noted above. Therefore, the average shaded area is $[1-(3\langle\theta\rangle/2\pi)-(\langle\gamma\rangle/2\pi)-b]V_b$. A simple evaluation for $\langle\gamma\rangle$ is $\langle\gamma\rangle\simeq\langle\theta\rangle/2$. Therefore, using $\langle\theta\rangle=\pi(a-b)$, we have for the shaded area the expression $[1-(7a/4)+3b/4)]V_b$. The cross-hatched area is bV_b. Particle 2 may fall in an area of size $\langle\theta\rangle V_b/\pi$ or $(a-b)V_b$. The total contribution of this configuration to T_3 is therefore

$$(T_3)_2=(a-b)[1-(7a/4)+(3b/4)+bf]\ . \tag{B6}$$

Case 3: Fig. 9(c). In this case $\beta u(1,2)=0$. If particle 3 falls in the shaded area $F(1,2,3)=1$; if it falls in the cross-hatched area $F(1,2,3)=f$; and if it falls in the black area $F(1,2,3)=f^2$. If the black area is Γ we have that $0\le\Gamma\le bV_b/2$, and hence $\langle\Gamma\rangle\simeq bV_b/4$. The cross-hatched area is about $[3b/2-\langle\Gamma\rangle]V_b$. The shaded area is about $(1-2a+\langle\Gamma\rangle)V_b$. Particle 2 may fall in an area which is approximately of size bV_b. The total contribution of this configuration to T_3 is therefore

$$(T_3)_3=b[1-2a+(b/4)+5bf/4+bf^2/4]\ . \tag{B7}$$

Case 4: Fig. 9(d). In this case $\beta u(1,2)=0$. If particle 3 falls in the shaded area $F(1,2,3)=1$; if it falls in the cross-hatched area $F(1,2,3)=f$. The average shaded area is $(1-2a)V_b$. The average cross-hatched areas is $2bV_b$. Particle 2 may fall in an area of size $(1-2a)V_b$. The contribution of this configuration to T_3 is therefore

$$(T_3)_4=(1-2a)[1-2a+2bf]\ . \tag{B8}$$

Summing up Eqs. (B5) to (B8), we finally obtain

$$T_3=[1-3a+(9a^2/4)+(ab/2)-(b^2/2)]+f[3b-(9ab/2)+3b^2/4]+f^2(5b^2/4)\ . \tag{B9}$$

For the three-dimensional case, we still use (B9) but with the appropriate values of a and b [see Eq. (21)].

The approximations we use to calculate T_3 are rather coarse, but the result is "self-consistent" in the sense that A_ϵ is not sensitive to the exact value of T_3, and the computer results are not sensitive to the exact value of A_ϵ. Therefore the above approximations are expected to be sufficient.

[1] A. Drory, I. Balberg, and B. Berkowitz, Phys. Rev. E **49**, R949 (1994).

[2] For a review, see I. Balberg, Philos. Mag. B **56**, 991 (1987).

[3] See, e.g., *Physics and Chemistry of Porous Media,* edited by D. L. Johnson and P. N. Sen (AIP, New York, 1984).

[4] A. L. R. Bug, S. A. Safran, G. S. Grest, and I. Webman, Phys. Rev. Lett. **55**, 1896 (1985); S. A. Safran, I. Webman, and G. S. Grest, Phys. Rev. A **32**, 506 (1985).

[5] J. Texeira, in *Correlations and Connectivity,* edited by H. E. Stanley and N. Ostrowsky (Kluwer Academic, Dordrecht, 1990), p. 167.

[6] D. H. Heyes and J. R. Melrose, J. Phys. A **21**, 4075 (1988).

[7] M. C. Barttelt and J. W. Evans, Phys. Rev. B **46**, 12675 (1992).

[8] A. Chhabra, D. Matthews-Morgan, D. P. Landau, and H. J. Herrmann, Phys. Rev. B **34**, 4796 (1986).

[8] D. Stauffer and A. Aharony, *Introduction to Percolation Theory* (Taylor and Francis, London, 1991).

[10] W. Haan and R. Zwanzig, J. Phys. A **10**, 1547 (1977).

[11] U. Alon, A. Drory, and I. Balberg, Phys. Rev. B **42**, 4634 (1990).

[12] A. Drory, I. Balberg, U. Alon, and B. Berkowitz, Phys. Rev. A **43**, 6604 (1991).

[13] I. Balberg and N. Binenbaum, Phys. Rev. A **35**, 5174 (1987).

[14] I. Balberg and N. Binenbaum, Phys. Rev. B **28**, 3799 (1983); I. Balberg, N. Binenbaum, and N. Wagner, Phys. Rev. Lett. **52**, 1465 (1984).

[15] T. deSimone, R. M. Stratt, and S. Demoulini, Phys. Rev. Lett. **56**, 1440 (1986).

[16] S. C. Netemeyer and J. D. Glandt, J. Chem. Phys. **85**, 6054 (1986).

[17] J. Xu and G. Stell, J. Chem. Phys. **89**, 1101 (1988).

[18] R. Kikuchi, J. Chem. Phys. **53**, 2713 (1970).

[19] J. Herterz, B. K. Chakrabarti, and J. A. M. S. Duarte, J. Phys. A **15**, L13 (1982).

[20] D. E. Sanders and J. W. Evans, Phys. Rev. A **38**, 4186 (1988); J. W. Evans, J. Phys. A **23**, L197 (1990).

[21] S. R. Anderson and F. Family, Phys. Rev. A **38**, 4198 (1988).

[22] For a general exposition and some applications, see *Monte Carlo Methods in Statistical Physics,* edited by K. Binder (Spring, Berlin, 1979), and references therein.

[23] H. Gould and I. Tobochnik, *An Introduction to Computer Simulation Methods* (Addison-Wesley, Reading, MA, 1988), Chap. 16 and references therein.

[24] M. Lagues, J. Phys. Lett. **40**, L331 (1979).

[25] I. Balberg, Phys. Rev. B **33**, 36 318 (1986).

[26] E. Cherlaix, E. Guyon, and S. Roux, Trans. Porous Media **2**, 31 (1987).

[27] A. S. Skal and B. J. Shklovskii, Fiz. Tekh. Poluprovodn. 7, 1589 (1973) [Sov. Phys. Semicond. 7, 1058 (1974)].
[28] J. Hoshen and R. Kopelman, Phys. Rev. B **14**, 3438 (1976).
[29] See, e.g., B Widom, J. Chem. Phys. **44**, 3888 (1966), and references therein.
[30] See, e.g., Hinrichsen, J. Stat. Phys. **44**, 793 (1986).
[31] J. P. Hansen and I. R. McDonald, *Theory of Simple Liquids,* 2nd ed. (Academic, London, 1986).
[32] K. Huang, *Statistical Mechanics* (Wiley, New York, 1963).
[33] D. Shanks, J. Math. Phys. **34**, 1 (1955); P. Wynn, Math. Tables Aids Comput. **10**, 91 (1956). For some uses, see M. V. Sangaranarayanan and S. K. Rangarayan, Chem. Phys. Lett. **101**, 49 (1983), and G. A. Baker and P. Graves Morris, *Padé Approximants* (Addison-Wesley, New York, 1981).
[34] S. Katsura, Phys. Rev. **115**, 1417 (1959); Phys. Rev. **118**, 1667 (1960).
[35] J. G. Kirkwood, J. Chem. Phys. **3**, 300 (1935).